Giant Halo at the Neutron Drip Line

J. Meng and P. Ring

Physik Department der Technischen Universität München, D-85747 Garching, Germany
(Received 2 December 1996)

Relativistic Hartree-Bogoliubov theory in coordinate space is used to describe the chain of zirconium isotopes reaching from ^{116}Zr to the drip line nucleus ^{140}Zr. Pairing correlations are taken into account by a density dependent force of zero range. For neutron numbers larger than the magic number $N = 82$ a giant neutron halo outside the core of ^{122}Zr is predicted. It is formed by up to six neutrons. [S0031-9007(97)04995-8]

The study of exotic nuclei far away from the line of β stability may cast new light on nuclear structure and novel and entirely unexpected features may appear: Neutron rich nuclei can have a structure very different from that of normal nuclei. They consist of a normal core surrounded by a skin of neutron matter. Close to the drip line, where the coupling to the continuum becomes important, a neutron halo can develop, as it has been observed in light nuclei, as, for instance, in ^{11}Li [1]. However, in all of the halos observed so far, one has only a very small number of neutrons, namely, one or two outside of the normal core. Even in the chain of He isotopes only ^{6}He shows indications of a possible halo containing two neutrons, whereas ^{8}He with its large two-neutron separation energy of 2.24 MeV has only a neutron skin [2].

In order to study the influence of correlations and many-body effects it would be very interesting to find also nuclei with a larger number of neutrons distributed in the halo. In this Letter we report on the theoretical prediction of a giant neutron halo for Zr isotopes close to the neutron drip line. It is formed by up to six neutrons outside of the ^{122}Zr core with the magic neutron number $N = 82$.

So far one has applied rather different techniques to describe halo phenomena in light nuclei [3,4], as, for instance, the exact solution of few-body equations treating inert subclusters as point particles, or the density dependent Hartree-Fock method in a localized mean field taking into account all the particles in a microscopic way, or full shell model diagonalizations based on oscillator spaces with two different oscillator parameters for the core and the halo particles. Recently, a fully self-consistent method has been developed. It is based on relativistic Hartree-Bogoliubov (RHB) theory in coordinate space [5]. It is a relativistic extension of conventional Hartree-Fock-Bogolyubov (HFB) theory in coordinate space [6]. Being relativistic it is able to take into account at the same time the proper isospin dependence of the spin-orbit term, which is very crucial for an accurate reproduction of recent measurements of the isotopic shifts in the Pb region [7] and for a reliable description of nuclei far away from the line of β stability [8]. In addition this theory provides a self-consistent treatment of pairing correlations in the presence of the continuum. As has been shown in Ref. [5] the scattering of Cooper pairs into the continuum containing low-lying resonances of small angular momentum plays an important role for the formation of a neutron halo. By using a density dependent zero range interaction, the halo in ^{11}Li has been successfully reproduced in this self-consistent picture. Very good agreement with recent experimental data has been obtained without any further adjustment of parameters. To obtain these results, a full solution of the RHB equations [9,10] in coordinate space is necessary.

The starting point is the relativistic mean field (RMF) Lagrangian

$$\mathcal{L} = \bar{\psi}\left(\not{p} - g_\omega\not{\phi} - g_\rho\not{\rho}\vec{\tau} - \frac{1}{2}e(1-\tau_3)\not{A} - g_\sigma\sigma - m\right)\psi + \frac{1}{2}\partial_\mu\sigma\partial^\mu\sigma - U(\sigma) - \frac{1}{4}\Omega_{\mu\nu}\Omega^{\mu\nu}$$

$$+ \frac{1}{2}m_\omega^2\omega_\mu\omega^\mu - \frac{1}{4}\vec{R}_{\mu\nu}\vec{R}^{\mu\nu} + \frac{1}{2}m_\rho^2\vec{\rho}_\mu\vec{\rho}^\mu - \frac{1}{4}F_{\mu\nu}F^{\mu\nu}. \tag{1}$$

It describes the nucleons with the mass m as Dirac spinors ψ moving in the fields of σ, ω, and ρ mesons and the Coulomb field. The field tensors for the vector mesons are given as $\Omega_{\mu\nu} = \partial_\mu\omega_\nu - \partial_\nu\omega_\mu$ and by similar expressions for the ρ meson and the photon. For a realistic description of nuclear properties a nonlinear self-coupling $U(\sigma) = \frac{1}{2}m_\sigma^2\sigma^2 + \frac{1}{3}g_2\sigma^3 + \frac{1}{4}g_3\sigma^4$ for the scalar mesons has turned out to be crucial [11].

In Ref. [9] relativistic Hartree-Bogoliubov equations are derived from such a Lagrangian:

$$\begin{pmatrix} h & \Delta \\ -\Delta^* & -h^* \end{pmatrix}\begin{pmatrix} U \\ V \end{pmatrix}_k = E_k\begin{pmatrix} U \\ V \end{pmatrix}_k, \tag{2}$$

where E_k are quasiparticle energies and the coefficients $U_k(r)$ and $V_k(r)$ are four-dimensional Dirac spinors. h is the usual Dirac Hamiltonian

$$h = \boldsymbol{\alpha}\boldsymbol{p} + g_\omega\omega + g_\rho\tau_3\rho + \beta(M + g_\sigma\sigma) - \lambda \tag{3}$$

containing the chemical potential λ adjusted to the proper particle number and the meson fields σ and ω determined as usual in a self-consistent way from the Klein Gordon equations in *no-sea* approximation.

The pairing potential Δ in Eq. (2) is given by

$$\Delta_{ab} = \frac{1}{2} \sum_{cd} V^{pp}_{abcd} \kappa_{cd} . \qquad (4)$$

It is obtained from the pairing tensor $\kappa = U^* V^T$ and the one-meson exchange interaction V^{pp}_{abcd} in the pp channel. More details are given in Ref. [9]. There it has been found that these forces are not able to reproduce even in a semiquantitative way proper pairing in the realistic nuclear many-body problem. As in Ref. [5] we therefore replace V^{pp}_{abcd} in Eq. (4) by the density dependent two-body force of zero range:

$$V(\boldsymbol{r}_1, \boldsymbol{r}_2) = \frac{V_0}{2} (1 + P^\sigma) \delta(\boldsymbol{r}_1 - \boldsymbol{r}_2) [1 - \rho(r)/\rho_0].$$
$$(5)$$

The RHB equations (2) for zero range pairing forces are a set of four coupled differential equations for the HB Dirac spinors $U(r)$ and $V(r)$. They are solved for the parameter set NLSH [12], which is widely used for the description of neutron rich nuclei, by the shooting method in a self-consistent way. The details will be published elsewhere. With a step size of 0.1 fm and using proper boundary conditions the above equations are solved in a spherical box of radius $R \geq 15$ fm. The results do not depend on the box size for $R \geq 20$ fm. For a radius $R = 30$ fm we found the same results within an accuracy of 0.1% for the binding energies and matter radius. Since we use a pairing force of zero range (5) we have to limit the number of continuum levels by a cutoff energy. For each spin-parity channel 20 radial wave functions are taken into account, which corresponds for $R = 20$ fm roughly to a cutoff energy of 120 MeV. For fixed cutoff energy and for fixed box radius R the strength V_0 of the pairing force (5) for the neutrons is determined by a calculation in the nucleus ^{116}Zr adjusting the corresponding pairing energy $-\frac{1}{2} \mathrm{Tr}\, \Delta\kappa$ to that of a RHB calculation using the finite range part of the Gogny force D1S [13]. For ρ_0 we use the nuclear matter density 0.152 fm^{-3}. In order not to miss any bound state the cutoff energy has to be larger than the depth of the potential. But as long as this is the case and as long as the interaction strength is properly renormalized, the results of this investigation stay practically unchanged. And in such a way, we get almost the same result from the pairing force of zero range and the finite range Gogny force.

We restricted our calculations to spherical shapes, because most of the investigations with nonrelativistic codes and with relativistic RMF + BCS codes show that the nuclei above ^{122}Zr are spherical. In addition there are investigations concerning the question of deformation in halo nuclei [14,15], in which it has been shown that halo nuclei are expected to be spherical.

In the upper panel of Fig. 1 we show the rms radii of the protons and neutrons for the zirconium isotopes with mass numbers $A = 110$ to $A = 140$, the drip line nucleus. To guide the eye we also give a dashed line with a $N^{1/3}$ dependence. It clearly shows a kink for the neutron rms radius at the magic neutron number $N = 82$.

These results can be understood more clearly by considering the microscopic structure of the underlying wave functions and the single particle energies in the canonical basis [16]. Therefore, in the lower panel of Fig. 1 we show the single particle levels in the canonical basis for the isotopes with an even neutron number. Going from $N = 70$ to $N = 100$ we observe a big gap above the $1h_{11/2}$ orbit. For $N > 82$, the neutrons are filled to the levels in the continuum or weakly bound states in the order of $3p_{3/2}$, $2f_{7/2}$, $3p_{1/2}$, $2f_{5/2}$, and $1h_{9/2}$.

The neutron chemical potential is given in Fig. 1 by a dashed line. It approaches rapidly the continuum already shortly after the magic neutron number $N = 82$ and it crosses the continuum at $N = 100$ for the nucleus to ^{140}Zr. In this region the chemical potential is very small and almost parallel to the continuum limit. This means that the additional neutrons are added with a very small, nearly vanishing binding energy at the edge of the continuum. The total binding energies E for the isotopes above ^{122}Zr are therefore almost identical. This has been recognized already in Ref. [8] in RMF calculations using the BCS approximation and an expansion in an oscillator basis, which is definitely not reliable for chemical potentials so close to the continuum limit. In the present investigation we obtain the same result treating now the continuum and its coupling to the bound orbits by pairing correlations properly within full relativistic HB theory in coordinate space.
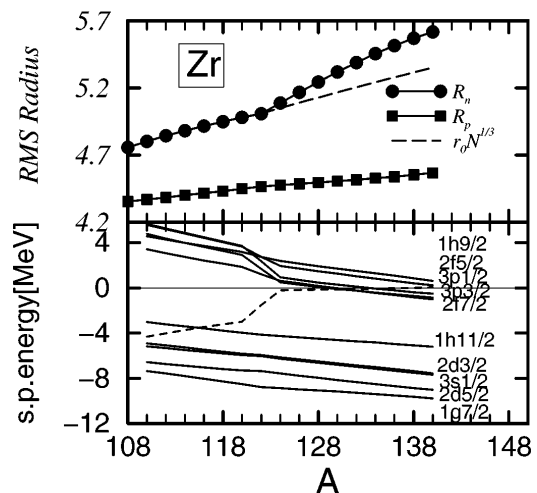

FIG. 1. Upper panel: rms radii for neutrons and protons in Zr isotopes close to the neutron drip line as a function of the mass number A. Lower panel: single particle energies for neutrons in the canonical basis. The dashed line indicates the chemical potential.

To understand the kink in the neutron rms radii shown in Fig. 1 we present in Fig. 2 the contributions $\langle r \rangle_{lj}$ of the different quantum numbers to these quantities. It is clearly seen that the radii for the negative parity levels close to the continuum limit are responsible for the rapid increase of the neutron radius. Neutrons above the closed neutron core $N = 82$ are filled into these orbits. As more and more neutrons are added, $3p_{3/2}$ and $2f_{7/2}$ (after $N > 88$), $3p_{1/2}$ (after $N > 92$), respectively, become weakly bound, then the contribution of further continuum $2f_{5/2}$ and $1h_{9/2}$ become more and more important. Going from $A = 122$ to $A = 140$ we observe an almost constant contribution of all the channels to the total rms matter radius except a sudden increase in the contribution of the $3p_{3/2}$, $2f_{7/2}$, $3p_{1/2}$, and $2f_{5/2}$ channels. This means that the giant halo in $^{124-140}$Zr are formed by the occupation of all these levels in the respective nucleus.

In the upper panel of Fig. 3 we show the corresponding density distribution for neutrons and protons in the nucleus ^{134}Zr. By dashed lines we show calculations for different values of the box size $R = 15, 20, 25$, and 30 fm. It is clear that we need very large box sizes to describe the halo properly. For $R = 30$ fm the neutron density is reliably reproduced only up to $r = 25$ fm, where it has decreased to 10^{-6} fm^{-3}. The full line in the upper panel of Fig. 3 is an asymptotic extension to infinite box size. On the other hand, the density distribution inside the nucleus is reproduced properly even for small values of the box size.

In the lower panel of Fig. 3 we show the relative contributions ρ_{nlj} of the different orbits characterized by the quantum numbers nlj with respect to the tot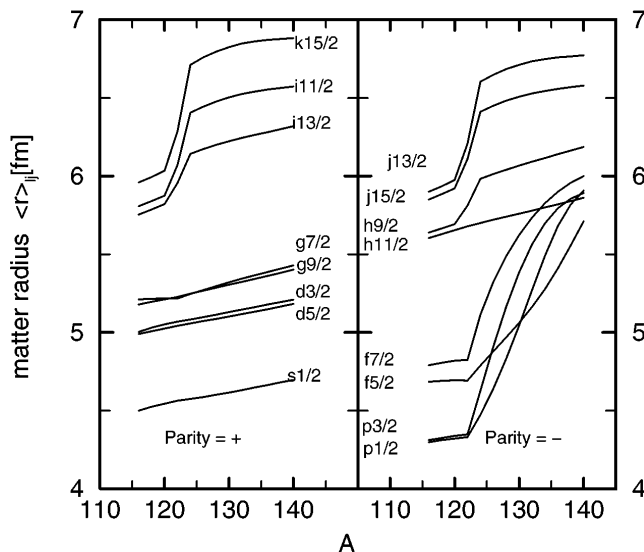al neutron density ρ_n. For comparison we also show the total neutron density in the shaded area in arbitrary units. As we see the halo is formed essentially by contributions from three orbits $3p_{3/2}$, $3p_{1/2}$, and $2f_{7/2}$. The most inner part of the halo ($7 \leq r \leq 9$ fm) the $2f_{7/2}$ orbit plays the dominant role. As can be seen in the lower part of Fig. 1, this orbit is slightly below the chemical potential and to the continuum limit in this nucleus. Further outside ($10 \leq r \leq 15$ fm) its relative contribution is strongly reduced because of the larger centrifugal barrier felt by the $l = 3$ orbit. In this region the orbit $3p_{3/2}$, which has nearly the same position as the $2f_{7/2}$ orbit, takes over. Because of the smaller orbital angular momentum, this orbit feels a reduced centrifugal barrier. For even larger distances from the center ($r \geq 15$ fm) its relative contribution is somewhat reduced and the $3p_{1/2}$ orbit gains importance. The $3p_{3/2}$ and the $3p_{1/2}$ levels feel the same centrifugal barrier, but the latter is situated directly at the continuum limit and therefore it is more loosely bound than the other two orbits.

In Fig. 4 we show for all the Zr isotopes between $A = 108$ and $A = 140$ the occupation probabilities in the canonical basis of all the neutron levels near the Fermi surface, i.e., in the interval $-20 \leq E \leq 10$ MeV. The chemical potential is indicated by a vertical line. For the mass numbers $A < 122$ the chemical potential lies several MeV below the continuum limit ($E = 0$) and there is only very little occupation in the continuum ($E > 0$). The nucleus ^{122}Zr has a magic neutron number and no pairing. As the neutron number goes beyond this closed core, the occupation of the continuum becomes
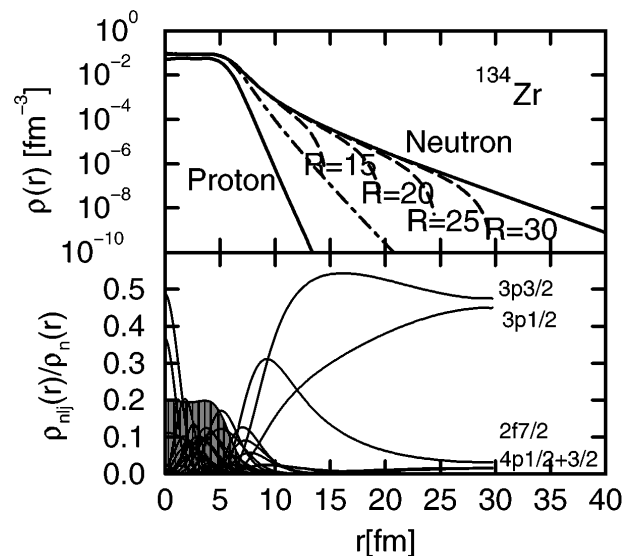

FIG. 2. Contributions $\langle r \rangle_{j\pi}$ for the different channels with the quantum numbers l and parity. The left panel show the orbits with positive parity and the right panel shows the levels with negative parity.

FIG. 3. Upper panel: neutron and proton density distribution in ^{134}Zr. Dashed lines indicate calculations for different values of the box size R and the dash-dotted line gives the neutron distribution for the core ^{122}Zr. Lower panel: relative contributions of the different orbits to the full neutron density as a function of the radius. The shaded area indicates the total neutron density in arbitrary units.
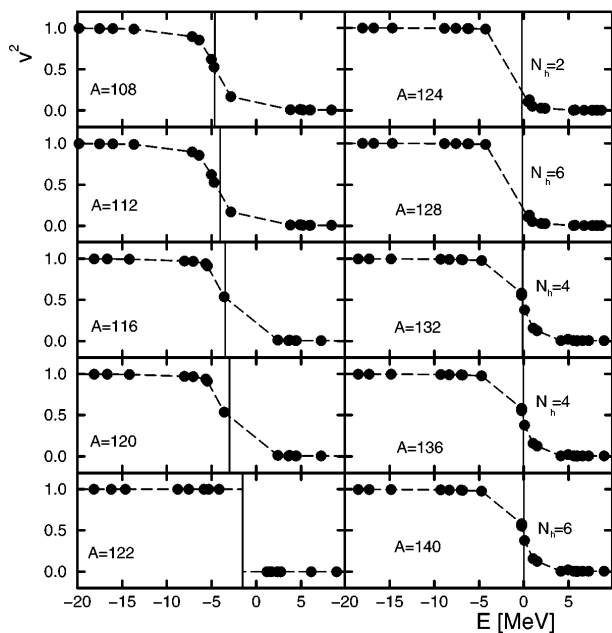
FIG. 4. The occupation probabilities in the canonical basis for various Zr isotopes with mass number A as a function of the single particle energy. The chemical potential is indicated by a vertical line. For $A > 122$ we also show the number N_h of neutrons in the halo.

more and more important. Adding up the occupation probabilities v^2 for the levels with $E > 0$ we find in the continuum two particles for $N = 84$, four for $N = 86$, six for $N = 88$, roughly three for $N = 90$, roughly four for $N = 92$, roughly three for $N = 94$, roughly four for $N = 96$, roughly five for $N = 98$, and roughly six for $N = 100$ (where the neutron drip line is reached).

Considering the very extended neutron rms radii of these systems and estimating the number of valence neutrons which would fit into the same volume outside the ^{122}Zr core (shown in Fig. 3 by a dash-dotted line) if they would be packed with normal neutron density, we find for ^{134}Zr 24 neutrons instead of 12 and for ^{140}Zr 34 neutrons instead of 18. This means that the density outside the ^{122}Zr core is reduced roughly by a factor of 2. This phenomenon is therefore clearly a neutron halo and not a neutron skin. As we see from Fig. 3 the tail of the density is proportional to $\exp(-2\sqrt{4mS}\,r)$ with $S \approx 0.4$ MeV. This fact is also emphasized by the extremely low $2n$-separation energies (<0.5 MeV) of these systems. We call this phenomenon a *giant halo* because of the large number of particles in the halo region.

Summarizing our investigations, we predict neutron halos in the Zr nuclei close to the neutron drip line, which

are composed not only of one or two neutrons, as is the case in the halos investigated so far in light p-shell nuclei, but which contain up to six neutrons. This is a new phenomenon, which has not been observed experimentally so far. It would allow the study of collective phenomena in neutron matter of low density. This prediction is based on relativistic Hartree-Bogoliubov theory in the continuum. It combines the advantages of a proper description of the spin-orbit term with those of full Hartree-Bogoliubov theory in the continuum, which allows in the canonical basis the scattering of Cooper pairs to low-lying resonances in the continuum. A density dependent force of zero range has been used in the pairing channel. It contains no free parameter, because its strength is adjusted for the isotope ^{116}Zr to a similar calculation with Gogny's force D1S in the pairing channel. The halos are formed by two to six neutrons scattered as Cooper pairs mainly to the levels $3p_{3/2}$, $2f_{7/2}$, $3p_{1/2}$, and $2f_{5/2}$. This is made possible by the fact that these resonances in the continuum come down very close to the Fermi level in these nuclei and by their coupling with the loosely bound levels just below the continuum limit.

[1] I. Tanihata *et al.,* Phys. Rev. Lett. **55**, 2676 (1985).
[2] G.D. Alkhazov *et al.,* Phys. Rev. Lett. **78**, 2313 (1997).
[3] J.M. Bang *et al.,* Phys. Rep. **264**, 27 (1996).
[4] M. Zhukov *et al.,* Phys. Rep. **231**, 151 (1993).
[5] J. Meng and P. Ring, Phys. Rev. Lett. **77**, 3963 (1996).
[6] J. Dobaczewski *et al.,* Nucl. Phys. **A422**, 103 (1984).
[7] M.M. Sharma, G.A. Lalazissis, and P. Ring, Phys. Lett. B **317**, 9 (1993); Phys. Rev. Lett. **74**, 3744 (1995).
[8] M.M. Sharma, G.A. Lalazissis, W. Hillebrandt, and P. Ring, Phys. Rev. Lett. **72**, 1431 (1994).
[9] H. Kucharek and P. Ring, Z. Phys. A **339**, 23 (1991).
[10] T. Gonzalez-Llarena, J.L. Egido, G.A. Lalazissis, and P. Ring, Phys. Lett. B **379**, 13 (1996).
[11] J. Boguta and A.R. Bodmer, Nucl. Phys. **A292**, 413 (1977).
[12] M.M. Sharma, M.A. Nagarajan, and P. Ring, Phys. Lett. B **312**, 377 (1993).
[13] J.F. Berger *et al.,* Nucl. Phys. **A428**, 32c (1984).
[14] I. Tanihata *et al.,* Nucl. Phys. **A583**, 769 (1995).
[15] T. Misu *et al.,* Nucl. Phys. **A614**, 44 (1997).
[16] P. Ring and P. Schuck, *The Nuclear Many-Body Problem* (Springer-Verlag, Heidelberg, 1980).